*Accepted for publication in* ***Lithuanian Journal of Physics*** *(2003).*

# MODELLING OF HTRs WITH Monte Carlo: SENSITIVITY DUE TO DIFFERENT ISOTOPIC FUEL COMPOSITION

**R. Plukienė[1*], D. Ridikas[2*], A. Plukis[1] and V. Remeikis[1]**

[1)]*Insitute of Physics,, Savanorių pr. 231, 2053 Vilnius, Lithuania*

[2)]*DSM/DAPNIA/SPhN, CEA Saclay, 91191 Gif-sur-Yvette, France*

* E-mail: rita@ar.fi.lt, ridikas@cea.fr

## ABSTRACT

The gas turbine modular helium-cooled reactor (GT-MHR) is a potential candidate for the maximum plutonium destruction in once-through cycle. A particular feature of GT-MHR is that its refractory coated fuel (TRISO particles) is supposed to provide an impermeable barrier to the release of fission products and, at the same time, to resist very deep burn-up rates (more than 90% for $^{239}$Pu). In this work we performed detailed simulations of GT-MHR operation by loading with different plutonium fuel vector: plutonium from military applicationns and plutonium from LWR and RBMK spent nuclear fuel. The comparison of the main GT-MHR performance parameters: $k_{eff}$ eigenvalues, the length of the fuel cycle, neutron characteristics and the evolution of fuel composition in particular were obtained for different plutonium isotopic vector. In all cases the same Monteburns (MCNP+ORIGEN) code system is used. We show that the performance of GT-MHR may be considerably influenced by the plutonium isotopic composition vector used as fuel material. This is the first time when transmutation possibility of the RBMK-1500 plutonium isotopic composition was tested using high temperature reactor.

*Keywords:* High temperature reactor, Monte Carlo simulation, incineration of plutonium.

## 1. INTRODUCTION

The gas turbine modular helium-cooled reactor (GT-MHR) is an advanced nuclear power plant that in principle could provide an increased safety, high thermal efficiency and deep burn-up rates [1]. The GT-MHR features are: the helium coolant, which is inert and remains in a single phase under all conditions; the graphite core, which provides high heat capacity, slow thermal response, and structural stability at high temperatures; the refractory coated particle fuel, which allows high burn-up, retains fission products during operation in high temperatures and retains their integrity in a repository environment for hundreds of thousands years. In principle, GT-MHR could be used to burn all types of fuel and offers significant advantages in accomplishing the transmutation of plutonium isotopes and high destruction of $^{239}$Pu in particular [2]. It utilizes natural erbium as burn-able poison with the capture cross section having a resonance at a neutron energy such that ensures a strong negative

temperature coefficient of reactivity. The lack of interaction of neutrons with coolant (helium gas) makes sure that temperature feedback of fuel and graphite is the only significant contributor to the power coefficient. As a matter of fact, no additional $^{239}$Pu is produced since no $^{238}$U is used (see section 3). A gas-cooled high temperature reactor or a separate irradiation zone in the centre of GT-MHR assembly, coupled to an accelerator [2,3], could also provide a fast neutron environment due to the same reason - the helium coolant is essentially transparent to neutrons and does not change neutron energies. Since fertile nuclei ($^{240}$Pu, $^{242}$Pu, $^{241}$Am, $^{243}$Am, $^{242}$Cm, $^{244}$Cm) have significant fission cross section in a fast neutron energy spectrum, one could consider an additional fast stage, following a thermal stage, in order to eliminate the remaining actinides [2,3].

A number of related studies have been made concerning the modelling of GT-MHR. The modelling of GT-MHR and plutonium based fuel cycles within a Monte Carlo approach have been performed by comparing ENDF, JEF and JENDL data libraries (Refs. [4], [5]). However, in these studies only a homogeneous geometry was considered. In Ref. [6] the critical GT-MHR loaded with Pu isotopes from military applications was investigated when comparing different geometry sets, namely homogeneous versus single-heterogeneous and double-heterogeneous using Monte Carlo. The similar problematic concerning the GT-MHR structure modelling and different fuel isotopic composition have been addressed in part in Ref. [7] but with different modelling schemes, i.e. a deterministic approach and/or based on the neutron diffusion theory.

In this paper we will describe in detail the use of a critical GT-MHR for transmutation of plutonium isotopes separated from LWR and RBMK-1500 spent nuclear fuel and plutonium from military applications. The main goal of our study is to compare the performance parameters of the reactor in the once-through cycle as a function of different fuel isotopic composition using double-heterogeneous reactor core geometry within Monte Carlo approach [6].

Monteburns [8], namely a coupled MCNP [9] and ORIGEN [10] code system, is employed at different stages of our simulations. The performance of it has been successfully benchmarked in Ref. [11] by simulating the fuel cycle of the high flux reactor at ILL Grenoble.

## 2. MODELLING DETAILS

The investigation of transmutation feasibility of different isotopic plutonium composition, separated from power reactor SNF (spent nuclear fuel), in GT-MHR reactor is based on 3D double-heterogeneous reactor core geometry with micro-particles as described in recent study [6]. Here we provide only a short description of the geometry modelling with MCNP, while further details on double heterogeneous geometry modelling can be found in Ref. 6.

The cross sectional view of the GT-MHR geometry is presented in Fig. 1. The annular active core is built up of 102 hexagonal graphite fuel columns located around the inner graphite reflector (37 columns) and reflector with $B_4C$ (24 columns). The core is enclosed by the blocks of side replaceable

and permanent graphite reflectors. They represent regular hexagonal prisms of 36 cm width across the flats and 80cm height. The top and bottom reflectors are placed above and below fuel assemblies arrangement, respectively. The main feature of double-heterogeneous geometry is a real active core structure: inside each hexagonal core column are 202 cylinders with fuel material, 14 cylinders with natural erbium and 108 cylinders with helium. Fuel and erbium cylinders also include ceramic - coated fuel and erbium particles mixed uniformly in a pressed graphite matrix. Each coated fuel particle consists of spherical kernel of $PuO_{2-x}$ surrounded by triple protective coatings from pyrocarbon and SiC (so called TRISO coating). The same structure is valid for particles containing burn-able poison - natural erbium in the form of $Er_2O_3$. We should note that the overall diameter of standard TRISO–coated particles may vary from 310 μm to about 850 μm [13]. The neutronics of the TRISO particle fuel is strongly affected by the fuel kernel size, especially for dimensions near the mean free path of resonance neutrons. In the case when the same material volume is preserved, the large diameter kernels will favor non-resonance neutron absorption, while small kernels will enhance resonance neutron absorption. In our calculations the smallest particle size with 200 μm fuel kernel diameter was taken. The enhanced resonance absorption of non-fissile plutonium component improves reactivity feedback and $k_{eff}$ stability especially in RBMK plutonium fuel case (see results in section 4). The civil plutonium (plutonium from power reactors SNF) core contains $3.18\times10^{10}$ particles, while military plutonium core - $1.87\times10^{10}$. Similarly as for fuel particles, erbium particles were placed in the burn-able poison channels. To fit the corresponding erbium mass for different fuel cases the number of Er particles in the compacts varies from $3.4\times10^{9}$ for military plutonium to $\sim1.5\times10^{8}$ for civil plutonium. The main parameters used for modelling of GT-MHR are summarized in Table 1.

In this work we used the MCNP code [9] to obtain k - eigenvalues and neutron fluxes. As soon as $k_{eff}$ is less than 1 the length of the fuel cycle is determined in the case of a critical system. In the more realistic description of GT-MHR, control rods would compensate the initial over reactivity. In our study the control rods were not designed since their effect would be very similar in the case of a comparative analysis (relative comparison) if modeled-omitted exactly in the same way for all fuel composition cases.

For burn-up calculations we employed the Monteburns code [8] in all cases. ENDF/B-VI data library (as the most often employed with MCNP) was used for the fuel and structure materials, JENDL-3.2 data files (having the biggest number of fission products) were employed for fission products.

Neutron spectrum in GT-MHR changes considerably during the fuel burn-up. A typical neutron spectrum evolution for low burn-up RBMK plutonium fuel with natural Er poison is shown in Fig. 2. The observed increase of the thermal flux from 9% to 22% is due to the burnout of $^{239}Pu$ and $^{240}Pu$ in addition to the loss of the burn-able poison during the operation for different fuel cases (see section 3). Indeed, the change of the energy spectra of neutrons will change the averaged cross sections to be

used in the burn-up calculations, in some cases by a factor of two or more [4]. Therefore, fuel evolution calculations have to be performed with corresponding variable neutron fluxes as it is done with Monteburns [9]. In this work the neutron fluxes and cross sections were recalculated in every fifty days for further ORIGEN burn-up calculations [10], since the neutron flux is dependent on the composition of the material.

We note also that at the constant reactor power typical averaged GT-MHR neutron fluxes in the active core may increase typically by 50-100 %, i.e. from ~$1\times10^{14}$ n/(cm$^2$ s) to ~$2\times10^{14}$ n/(cm$^2$ s) at the beginning and at the end of the fuel cycle respectively [4].

## 3. INPUT DATA

As it was mentioned above, our major interest in this study was to look at the GT-MHR performance parameters by investigating different plutonium fuel isotopic configuration, i.e. plutonium originating from: a) the spent nuclear fuel of LWR (light water reactor), b) the spent nuclear fuel of RBMK - 1500 (graphite - moderated water - cooled reactor), and c) plutonium found in military applications (mainly Pu-239, 240 and 241).

The initial fuel and burn-able poison compositions are presented in Table II. Plutonium from LWR reactor (LWR Pu) was composed of: 2.7 % of $^{238}$Pu, 55.08 % of $^{239}$Pu, 23.08 % of $^{240}$Pu, 11.83 % of $^{241}$Pu and 7.3 % of $^{242}$Pu. It is plutonium from 42 MW d/kg burn-up LWR SNF after 5 years of cooling time [8]. In the case of military plutonium (Military Pu) the following isotopic vector was taken: 94.0 % of $^{239}$Pu, 5.4 % of $^{240}$Pu and 0.6 % of $^{241}$Pu [8].

As long as the RBMK plutonium is concerned– its isotopic composition strongly depends on the initial $^{235}$U enrichment of reactor fuel and its final burn-up conditions. The fuel burn-up distribution of the accumulated Ignalina NPP spent nuclear fuel assemblies in the unit 1 and 2 cooling pools is given in Fig.2 [14]. It is nearly half of the total amount of SNF to be accumulated during reactor's operation time. To obtain the expected situation after 50 years (foreseen time for intermediate storage) four different burnup and $^{235}$U enrichment RBMK-1500 reactor spent fuel composition were calculated using SCALE 4.4a code package [15, 16]. The fuel isotopic composition evaluation method using SCALE 4.4a has been validated in part by gamma spectrometry experiments with the Pu sources of different burnup rates [17]. The following plutonium compositions were selected for the initial loading in GT-MHR (see Table 2.):

- RBMK Pu1 – 2% $^{235}$U initial enrichment, 14MWd/kg burnup plutonium composition was : 0.2% $^{238}$Pu, 66.8 % $^{239}$Pu, 30.2 % $^{240}$Pu, 0.7 % $^{241}$Pu and 2.1 % $^{242}$Pu ;
- RBMK Pu2 – 2% $^{235}$U initial enrichment, 20MWd/kg burnup plutonium : 0.5% $^{238}$Pu, 56.1 % $^{239}$Pu, 36.9 % $^{240}$Pu, 1.0 % $^{241}$Pu and 5.4 % $^{242}$Pu ;

- RBMK Pu3 – 2.4% $^{235}$U initial enrichment, 22MWd/kg burnup plutonium : 0.6% $^{238}$Pu, 57.1 % $^{239}$Pu, 35.8 % $^{240}$Pu, 1.1 % $^{241}$Pu and 5.4 % $^{242}$Pu ;
- RBMK Pu4 – 2.6% $^{235}$U initial enrichment, 26MWd/kg burnup plutonium: 0.8% $^{238}$Pu, 54.4 % $^{239}$Pu, 36.6 % $^{240}$Pu, 1.2 % $^{241}$Pu and 7.1 % $^{242}$Pu.

Uranium fuel with a 2% enrichment was used from the very beginning of INPP operation. It is the same type of fuel loaded in RBMK-1000 reactors in Chernobyl (Ukraine). We have chosen two SNF burn-up cases with this enrichment: 1) 14 MWd/kg - assemblies of low burn-up and 2) 20MWd/kg - assemblies of high burn-up, both representative for a typical burn-up fuel before 1996. From 1996 up to now the 2.4% $^{235}$U enrichment fuel with 0.41% burnable poison (erbium) is the most frequently used nuclear fuel in RBMK-1500; here the average fuel burn-up is 22MWd/kg. The last RBMK Pu4 case was selected to test the SNF originated from new nuclear fuel (2.6% $^{235}$U enrichment and 0.5% of burnable poison – erbium, which was first tested in Ignalina INPP in ~2001. This initial fuel load characteristic most probably will not change very much until Ignalina NPP shutdown (first unit in 2004 and second unit in 2009). The corresponding GT-MHR plutonium fuel masses are presented in Table 2. 1200 kg for civil plutonium cases and 700 kg for military plutonium were the optimized fuel quantities for GT-MHR. The burnable poison erbium in natural isotopic composition was added to reactor core to achieve the same $k_{eff}$ eigenvalue at the beginning of the fuel cycle for LWR Pu, RBMK Pu1 and Military Pu. The high amount of $^{240}$Pu in other three cases Pu2, Pu3 and Pu4 limited the possibility to add burnable poison (see 4 section).

## 4. RESULTS

We perform our calculations by simulating the once-through fuel cycle scenario at the constant 600 $MW_{th}$ power. The length of the fuel cycle is determined according to the following criterion: $k_{eff} \geq 1$ within statistical errors. The first task was to check the suitability of the RBMK plutonium as a potential GT-MHR fuel. For this purpose GT-MHR performance parameters were analyzed for four RBMK fuel cases without burnable poison. The $k_{eff}$ eigenvalues as a function of time (consequently, as a function of burn-up) for RBMK Pu1, Pu2, Pu3 and Pu4 compositions are presented in Fig. 4. The highest $k_{eff}$ at the beginning (1.156±0.006) and later on was obtained for RBMK Pu1 case. Such result was expected taking into account a favourable plutonium isotopic composition: about 10% bigger amount of $^{239}$Pu and less $^{240}$Pu quantity caused the increase in $k_{eff}$ by $\Delta k_{eff} = 0.05$ comparing with other cases. For the other three cases: RBMK Pu2, RBMK Pu3 and RBMK Pu4 $k_{eff}$ begins at 1.087, 1.103 and 1.088 correspondingly (with $1\sigma$=0.006 in all cases). Without burnable poison the shortest fuel cycle - 800 days was estimated for RBMK Pu4, for the RBMK Pu3 and RBMK Pu2 fuel cycle length was approximately the same ~900 days, and the longest fuel cycle was obtained for RBMK Pu1 case. RBMK Pu1 isotopic composition has demonstrated the best GT-MHR performance.

As far as RBMK Pu2, Pu3 an Pu4 cases do not differ very much from the point of view of isotopic composition and $k_{eff}$ behavior for the full comparative analysis of the different plutonium vector further we present only calculation results for the following four cases: Military Pu, LWR, RBMK Pu1 and RBMK Pu3.

The GT-MHR with military plutonium composition was tested in our previous study [7]. In order to obtain relative fuel cycle length for different GT-MHR fuel cases the appropriate quantity of burnable poison was added to achieve the same starting $k_{eff}$. Unfortunately RBMK Pu3 $k_{eff}$ was too low at the beginning and it was impossible to add burnable poison, but RBMK Pu1 composition with burnable poison was compared with the LWR Pu and military Pu. Fig. 5 presents $k_{eff}$ as a function of time for these three cases.

For military Pu case $k_{eff}$ begins at 1.132±0.006 and sharply decreases. Such $k_{eff}$ behaviour is related to fast $^{239}$Pu disappearance. Despite the significant amount of burn-able poison erbium (see Table 2) used to suppress intensive plutonium burning and to stabilize $k_{eff}$, the fuel cycle length holds only for ~550 days. This could be explained by particular erbium channel geometry and enhanced self-shielding effect in the small erbium particles. The fact what erbium material particles are placed in the heterogeneous channels at certain position in the fuel assembly (only 14 cylinders with natural erbium to 202 of fuel in the GT-MHR assembly) changes a lot the reactor parameters comparing them if it would be distributed homogeneously in all active core volume - the detailed demonstration of it was done in Ref. 7. Despite the tiny micro-particle size the self-shielding effect is present for plutonium ($PuO_2$) and erbium ($Er_2O_3$) cases with high material density: the local neutron flux is depressed inside the particle volume due to neutron absorption near the surface of the material. This is especially important at resonance energies, where the absorption cross sections are large as in case of $^{167}$Er, $^{239}$Pu, $^{241}$Pu and particularly $^{240}$Pu.

In the LWR plutonium case $k_{eff}$ starts at the 1.138±0.006, later $k_{eff}$ curve is constantly decreasing and drops below 1 approximately after 850 days. When erbium was added in RBMK Pu1 case the $k_{eff}$ at the beginning of fuel cycle was obtained 1.132±0.006. One can observe what in RBMK Pu1 case the decrease of $k_{eff}$ is slightly slower in the first part of GT-MHR operation; in addition, the fuel cycle is significantly longer - 1100 days if compared to LWR Pu. At the first step (50 days) of operation in both civil plutonium cases $k_{eff}$ decreases by ~0.02 (in RBMK Pu1 case even 0.03) due to the intense $^{239}$Pu burning; later due to the formation of fissile $^{241}$Pu this decrease becomes slower (see Fig. 5 for details). Different quantities of $^{240}$Pu (amount of $^{240}$Pu in RBMK Pu1 case is 1.3 times bigger) determine somewhat different behavior of $k_{eff}$ in these two cases. In the case of RBMK Pu1 the loss of fissile $^{239}$Pu is compensated by formation of $^{241}$Pu, therefore $k_{eff}$ remains rather stable up to 500 days and decreases somewhat faster later on as a function of both $^{239}$Pu and $^{241}$Pu burn-up. In Fig. 4 one can observe the same phenomenon for other RBMK fuel cases, where is no erbium in the system at all. In this case no burnable poison influence on $^{239}$Pu burning and consequently on $k_{eff}$ is seen, i.e. GT-MHR with RBMK fuel can support operating itself and the TRISO fuel kernel is of

right dimensions to provide stable $k_{eff}$ by enhanced resonance neutron absorption of fertile nucleus like $^{240}$Pu.

Even more - the absence of burnable poison in RBMK Pu3 case do not change the reactivity feedback - the negative $\Delta k_{eff}/\Delta T$ values in the GT-MHR were obtained for fuel, graphite and both fuel and graphite temperature increase as it is shown in Table 3. Negative reactivity coefficients were observed for RBMK Pu1 and LWR Pu cases with erbium poison. The biggest amount of Er was in Military Pu case. Natural erbium contains about 23% of $^{167}$Er, which has pronounced absorption resonance at the neutron energy of about 0.5 eV (see Fig. 6B). The presence of Er determines the absorption of neutrons when temperature (consequently the neutron energy too) of the core increases and in such way helps to ensure negative reactivity feedback. Otherwise its role because of self-shielding effect in the particles and special Er channel geometry is limited. For Military Pu case with fuel temperature increase (from 1200 K to 1500 K, when $T_{Graphite}$=const.) the reactivity coefficient is not negative but statistically is not significant, possibility to increase calculation precision further is limited by nuclear data accuracy and complicated geometry modeling. When influence of graphite or both fuel and graphite temperature increase in military Pu case was analyzed, the negative reactivity coefficients were obtained (see Table 3).

The neutron absorption by fuel material or by erbium is defined by thermal and resonance neutron flux, microscopic cross-sections of each nuclide and isotope atomic density in the system.

To explain the $k_{eff}$ behavior and plutonium evolution the effective macroscopic cross-sections were used. The effective macroscopic cross sections for entire system were obtained in the following way: $\Sigma_i^{(\alpha)}[\mathrm{cm}^{-1}] = 10^{-24} N_i \sigma_i^{(\alpha)}[\mathrm{b}]$, where $N_i$ - number of nuclei $i$ per unit volume [cm$^{-3}$], $\sigma_i^{\alpha}$ - one energy group microscopic cross-section of type $\alpha$ [barns] (fission, absorption, scattering) of nucleus $i$. The mean free path for $\alpha$ reaction is simply: $\Lambda^{(\alpha)} = 1/\Sigma^{(\alpha)}$.

The effective microscopic and effective macroscopic capture/fission cross-sections at different burn-up stages for main plutonium isotopes and $^{167}$Er in different GT-MHR fuel cases are presented in Table 4 (for Military Pu), Table 5 (for LWR), Table 6 (for RBMK Pu1) and Table 7 (RBMK Pu3).

Self shielding effect for $^{239}$Pu and $^{241}$Pu is not very significant for all considered GT-MHR fuel cases as it is demonstrated in terms of the microscopic capture and fission cross sections in Tables 4, 5, 6, 7. When self shielding effect is negligible the effective macroscopic cross sections correlate with the isotope quantities in each case (see Table 2 and Tables 4-7 for comparison). For example, the little amount of $^{241}$Pu in military plutonium case determines the small effective macroscopic cross-sections values at the beginning of fuel cycle and the growth of the values at the EFC.

The effective macroscopic $^{240}$Pu capture cross sections do not differ very much in civil plutonium cases (see Tables 5, 6 and 7) as it would be expected from the significant differences in isotopic composition between LWR, RBMK Pu1 and RBMK Pu3 cases. This could be explained by the large neutron capture resonance of $^{240}$Pu at the neutron energy of 1.0 eV. If the same fuel particle

size is considered, certain $^{240}$Pu quantity is sufficient to absorb the most of the resonance neutrons already in the first mean free path kernel layer (for $^{240}$Pu RBMK Pu1 ~100 μm, RBMK Pu2 ~90 μm). In the case of military plutonium at the beginning neutron absorption by $^{240}$Pu is smaller due to smaller initial mass of this isotope (accordingly smaller effective macroscopic capture cross section). At the end of the fuel cycle, the mass of $^{240}$Pu increases, while $\sigma_{capt}$ decreases, and $\Sigma_{capt}$ approaches to similar values as in the case of civil plutonium (Tables 4, 5, 6, 7).

The microscopic capture cross-sections for $^{167}$Er shown in Table 4 are smaller compared to RBMK Pu1 (Table 6) and LWR Pu (Table 5) cases. This is due to a significant self shielding in Er particles. The smaller Er microscopic cross section results in a smaller effective macroscopic cross-section with respect to civil plutonium cases.

In Fig. 6 we presented averaged neutron fluxes in micro-particles for all isotopic fuel composition considered both in the beginning (BFC) and at the end of the fuel cycle (EFC). Neutron fluxes "seen" by Pu and Er particles are presented in separate graphs on the left (6A) and on the right (6B) respectively. In all cases the same fission power was hold. It is clearly seen that at the beginning a thermal neutron contribution in fuel material is similar in LWR (~8.8%), RBMK Pu1 (~9%), RBMK Pu3 (~9.6%) and military plutonium (~10 %) cases. Small differences in first two cases are due to different amount of plutonium and different isotopic composition (see Table 2). In the RBMK Pu3 case thermal flux is not suppressed by erbium comparing with the LWR Pu and RBMK Pu1 cases. Slightly higher thermal neutron flux in military plutonium case is due to less overall fuel material mass - 700 kg (and number of particles respectively) including the self shielding of erbium in the burnable poison particles – these circumstances result in smaller thermal neutron absorption.

One can observe that in the resonance region neutrons are equally suppressed by the presence of $^{240}$Pu in civil plutonium cases both at the beginning and at the end of irradiation cycle. This is an illustration of the above statement that a certain quantity of $^{240}$Pu is sufficient to absorb nearly all resonance neutrons in the first mean free path layer. The neutron absorption at resonance 0.3 eV in $^{239}$Pu is also seen in Fig. 6, and it decreases with time due to $^{239}$Pu burn-up at the end of the fuel cycle. In civil plutonium cases resonance capture of 2.67 eV energy neutron of $^{242}$Pu is observed (Fig. 6 A). At the end of irradiation the bigger quantity of $^{242}$Pu is accumulated and the neutron absorption in resonance region is more pronounced.

The neutron flux spectrum presented in Fig. 6B shows, that at the beginning the most intensive neutron resonance capture in erbium particles is in military plutonium case. It is determined by almost 8 times bigger Er mass and somewhat higher thermal neutron flux when compared to other cases. Neutron flux spectrum in Er particles in both civil plutonium cases is similar (Fig. 6B). In the civil plutonium cases no erbium is left at the EFC. Contrary in HTR with military plutonium fuel there are still ~20kg of erbium left at EFC, and therefore thermal neutrons are suppressed in erbium resonance region.

Plutonium evolution for Military Pu, LWR Pu, RBMK Pu1 and RBMK Pu3 cases is presented in Fig. 7. The main plutonium isotope evolution for different cases are proportional to the effective macroscopic cross sections, which at the same time serve as isotope destruction or formation decline or growth coefficients (if neutron flux is constant) (see Tables 4 to 7 for details). The fastest burn-up of $^{239}$Pu was obtained in the Military Pu case, the slowest one - in the LWR Pu case. We also note significant differences for the $^{240}$Pu and $^{241}$Pu evolution. In military plutonium case the production of $^{240}$Pu from $^{239}$Pu is most intensive simply because $^{239}$Pu dominates the fuel isotopic composition. The greatest $^{240}$Pu destruction and $^{241}$Pu formation was in RBMK Pu3 case – this means that self-shielding effect occurred in fuel particle kernel helped to hold the neutron balance and that these particle dimensions are favorable for RBMK plutonium fuel transmutation in GT-MHR. The same is valid also for RBMK Pu2 and Pu4 cases.

As long as the total fuel burn-up is concerned, RBMK Pu1 seems to be the most attractive (see Table 8). GT-MHR loaded with RBMK Pu1, when compared with the LWR and military plutonium loads, gives the longest fuel cycle, i.e.1100 days, 850 days and 550 days respectively. In addition, a very efficient $^{239}$Pu burn-up (93%), and relatively small accumulation of minor actinides at the end of the fuel cycle is obtained in this particular case. For RBMK Pu1 56% of the initial plutonium has been burned, for Military Pu - 48%, and for LWR Pu - 43%. RBMK Pu3 plutonium without burnable poison also showed good performance parameters of GT-MHR – transmutation of $^{239}$Pu is 90% and about 48% of all plutonium. We note that these burnup rates still could be improved with the help of some dedicated fuel shuffling strategies. Studies along these lines should be definitely continued.

The masses of other actinides at the end of the fuel cycle are given explicitly in Table 8. The accumulation of minor actinides is approximately the same for all civil plutonium cases (7.5% for LWR Pu and RBMK Pu 3 cases, 6.8% for RBMK Pu1) and small in military plutonium case (~1%).

Finally we note that after the decommissioning of the Ignalina NPP about 22.5 tons of plutonium will be accumulated in the SNF. In practice, one would need 2 GT-MHR units with 10 fuel loads every 3 years (assuming that reactor's life is ~30 years) to burn all INPP SNF plutonium. The outcome of the once-through GT-MHR fuel cycle of RBMK plutonium transmutation would be ~127 TWh of electric power.

## CONCLUSIONS

A critical GT-MHR reactor dedicated to burn plutonium isotopes in the once-through fuel cycle was studied comparing its performance parameters as a function of different isotopic fuel composition: military plutonium, plutonium extracted from LWR and RBMK spent nuclear fuel. The possibility to transmute the RBMK-1500 plutonium separated from SNF in high temperature helium cooled reactor was investigated for the first time. We have shown that the performance of the system (e.g., $k_{eff}$, its

behavior with time and the length of the fuel cycle) during the fuel cycle will strongly depend on the initial plutonium isotopic composition. The following conclusions are drawn:

1. A significant difference was found in $k_{eff}$ evolution as a function of burn-up, in length of the fuel cycle and in the transmutation efficiency between military, LWR, and RBMK plutonium cases. Starting at the same $k_{eff}$ value, military plutonium $k_{eff}$ is decreasing continuously and already after 550 days the fuel cycle ends with 73% burn-up of $^{239}$Pu. LWR fuel cycle continues 850 days and 82% of the $^{239}$Pu burn-up is obtained. GT-MHR performance with 14MWd/kg RBMK plutonium is even better: longer fuel cycle (1100 days), very efficient $^{239}$Pu burning (93%) and relatively small accumulation of minor actinides at the end of the fuel cycle.
2. Thermal neutron contribution to neutron flux spectrum at the beginning of the fuel cycle inside TRISO fuel particles is quite similar, i.e. 9-10% for all cases considered. The observed increase of the thermal flux at the end of the fuel cycle increases up to 22%.
3. It seems that TRISO fuel kernels are of right dimensions to provide negative temperature coefficient by enhanced resonance neutron absorption of $^{240}$Pu nucleus in RBMK and LWR fuel cases. The same is valid for the core loaded with military plutonium
4. The most attractive RBMK plutonium composition is that of 14MWd/kg burn-up (up to now about 15% from all RBMK SNF), but the use of other burn-up RBMK SNF plutonium in GT-MHR is also possible. In 22 MWd/kg burn-up RBMK plutonium case 90% of $^{239}$Pu transmutation rate was obtained. GT-MHR, loaded with plutonium originating from RBMK, due to higher amount of $^{240}$Pu can support rather long operation time thanks to the formation of $^{241}$Pu which compensates the decrease of $^{239}$Pu. In addition, fuel load without burnable poison (22 MWd/kg burn-up RBMK plutonium case) does not affect the GT-MHR safety as long as its temperature coefficient is concerned – it remains negative in all cases.
5. In practice, one would need 2 GT-MHR units with 10 fuel loads every 3 years (assuming that reactor's life is ~30 years) to burn all INPP SNF plutonium. The outcome of the once-through GT-MHR fuel cycle of RBMK-1500 plutonium transmutation would be ~127 TWh of electric power.

Finally we note that the above burn-up rates still could be improved with the help of some dedicated fuel shuffling strategies. Studies along these lines should be definitely continued.

## ACKNOWLEDGEMENTS

This work was in part supported by the French-Lithuanian cooperation program "Gilibert".

**REFERENCES**

[1] Conceptual Design Description Report: Gas Turbine-Modular Helium Reactor (GT-MHR), No. **910720**, Revision 1, General Atomics, GA Project No.7658, (San Diego, USA, 1996).

[2] C. Rodriguez, A. Baxter et al., Deep-Burn: Making Nuclear Waste Transmutation Practical, Nuclear Engineering and Design **2805**, 1-19 (2003).

[3] A. Baxter, C.Rodriguez, M. Richards, J. Kuzminski, Helium-Cooled Reactor Technologies for Accelerator Transmutation of Nuclear Waste, in: *Proc. of the 6th OECD/NEA Information Exchange Meeting on Actinide and Fission Product Partitioning and Transmutation*, (Madrid, Spain, 2000) paper 72, pp. 593-609.

[4] D. Ridikas, G. Fioni, P. Goberis, O. Deruelle, M. Fadil, F. Marie, Critical and Sub-Critical GR-MHRs for Waste Disposal and Proliferation-Resistant Plutonium Fuel Cycles, in: *Proceedings of the 6th OECD/NEA Information Exchange Meeting on Actinide and Fission Product Partitioning and Transmutation,* (Madrid, Spain, 2000) paper 71, pp. 917-927.

[5] D. Ridikas, L. Bletzacker, O. Deruelle, M. Fadil, G. Fioni, A. Letourneau, F. Marie, R. Plukiene, Comparative Analysis of ENDF, JEF and JENDL Data Libraries by Modelling High Temperature Reactors and Plutonium Based Fuel Cycles: Military Pu case, in: *Proceedings of the Int. Conference on Nuclear Data for Science and Technology (ND2001)*, (Tsukuba Japan, 2001); Nucl. Science and Technology, 1049-1052 (2002).

[6] D. Ridikas, L. Bletzacker, O. Deruelle, M. Fadil, G. Fioni, A. Letourneau, F. Marie, R. Plukiene, Comparative Analysis of Different Data Libraries for the Performance of High Temperature Reactors (GT-MHR): Civil Pu case, in: *Proceedings of the Int. Conference on Accelerator Applications/Accelerator Driven Transmutation Technology and Applications (AccApp/ADTTA'01)*, (Reno, Nevada, USA, 2001).

[7] R. Plukiene and D. Ridikas, Modelling of HTRs with Monte Carlo: from a Homogeneous to an Exact Heterogeneous Core with microparticles, Annals of Nuclear Energy **30** (15), 1573–1585 (2003).

[8] F. Damian, Capacity Analysis of HTRs in terms of utilisation of fissile materials, report **CEA-R-5981** (PhD thesis in French), CEA Saclay (2001); F. Damian, X. Raepsaet, F. Moreau, Code and Methods Improvement in HTGR Modelling at CEA, in: *Proceedings of the Int. Conference PHYSOR 2002*, (Seoul, Korea, 2002) pp. 5A-03.

[9] H. R. Trellue and D.I. Poston, User's Manual, Version 2.0 for Monteburns, Version 5B, preprint **LA-UR-99-4999,** LANL (1999).

[10] J.F. Briesmeister, MCNP - A General Monte Carlo N-Particle Code, Technical Report **LA-12625-M**, LANL (1997).

[11] RSIC Computer Code Collection, ORIGEN 2.1 - Isotope Generation and Depletion Code Matrix Exponential Method, RSIC report **CCC-371** (1991).

[12] D. Ridikas, O. Deruelle, M. Fadil, G. Fioni, P. Goberis, F. Marie, On the Fuel Cycle and Neutron Fluxes of the High Flux Reactor at ILL Grenoble, in: *Proceedings of the 5th Int. Specialists Meeting SATIF-5, OECD/NEA*, (Paris, France, 2000) pp.383-393.

[13] M. P. Labar, The Gas Turbine – Modular Reactor: Promising option for Near Term Deployment, **GA-A23952**, (2002).

[14] I. Kirov, V. Sheider, Nuclear fuel management at INPP, current status, in: *Proceedings of Spent Fuel Management Workshop*, (Visaginas-Vilnius, Lithuania, 2003).

[15] S. M. Bowman and L. C. Leal, ORIGEN-ARP: Automatic Rapid Process for Spent Fuel Depletion, Decay, and Source Term Analysis, **ORNL/NUREG/CSD-2/V1/R6**, (2000).

[16] O. W. Hermann, C. V. Parks, SAS2H: A Coupled One-Dimensional Depletion and Shielding Analysis Module, **ORNL/NUREG/CSD-2/V2/R6**, (2000).

[17] E. Kimtys, A. Plukis, R. Plukiene, G. Braziunas, P. Goberis, A. Gudelis, R. Druteikiene and V. Remeikis, Analysis of Plutonium Isotopic Ratios Using the Scale 4.4A Code Package, Environmental and Chemical Physics*,* **22** (3-4), 112-116 (2001).

*Accepted for publication in* ***Lithuanian Journal of Physics*** *(2003).*

# AUKŠTATEMPERATŪRIŲ REAKTORIŲ MODELIAVIMAS: SKIRTINGOS KURO IZOTOPINĖS SUDĖTIES ĮTAKA

Modulinis heliu aušinamas aukštatemperatūris reaktorius (GT-MHR) yra vienas iš kandidatų idealiai tinkančių $^{239}$Pu transmutacijai [1]. Reaktoriaus ypatumas – kuro elemento konstrukcija (0.2 mm diametro kuro dalelės, padengtos aukštai temperatūrai atsparios keramikos sluoksniais TRISO) lemianti aukštas kuro išdegimo vertes (>90% $^{239}$Pu) ir tuo pačiu užtikrinanti labai mažą kuro elemento išsihermetinimo tikimybę. Aukštatemperatūriame reaktoriuje varijuojant neutronų spektro parametrais galima naudoti įvairų branduolinį kurą [2]. Šiame darbe nagrinėjama pradinės reaktoriaus kuro sudėties įtaka GT-MHR reaktoriaus eksploataciniams parametrams. Kaip reaktoriaus kuras naudojamas plutonis išskirtas iš LVR ir RBMK reaktoriaus naudoto branduolinio kuro (NBK) bei karinis plutonis. Nustatyta $k_{eff}$ kitimas reaktoriaus darbo metu, kuro ciklo trukmė, neutronų spektro kitimas aktyviojoje zonoje, kuro sudėties evoliucija bei atliekų izotopinė sudėtis. Modeliavimas ir skaičiavimai atlikti Monteburns (MCNP+ORIGEN) kodų sistema [3]. Parodyta, kad GT-MHR veikimui svarbus veiksnys yra pradinė plutonio izotopinė sudėtis kure. Šiame darbe pirma kartą buvo ištirta plutonio, išskirto iš RBMK-1500 NBK, transmutavimo galimybė aukštatemperatūriame reaktoriuje.

**Table 1.** Basic GT-MHR parameters.

| | |
|---|---|
| Power, $MW_{th}$ | 600 |
| Active core size: | |
| - height, cm | 800.0 |
| - area, $m^2$ | 11.5 |
| Active core volume, $m^3$: | 91.9 |
| Graphite mass in reactor, t: | 616.3 |
| Averaged temperature, $^oC$: | |
| - active core | 800 |
| - inner reflector | 730 |
| - side, top and bottom reflectors | 500 |

**Table 2.** Different GT-MHR fuel and erbium load at the beginning of the fuel cycle considered in this work. *Note, that in RBMK Pu1 case GT-MHR performance parameters where investigated two times – with burnable poison erbium (Fig. 5), and without erbium (Fig. 4).

| Fuel | Military Pu | LWR Pu | RBMK Pu1* | RBMK Pu2 | RBMK Pu3 | RBMK Pu4 |
|---|---|---|---|---|---|---|
| Isotopic Pu composition, kg | | | | | | |
| $^{238}$Pu | -- | 32.4 | 2.5 | 6.0 | 7.0 | 9.5 |
| $^{239}$Pu | 659.0 | 661.0 | 802.1 | 673.3 | 685.5 | 652.2 |
| $^{240}$Pu | 37.8 | 277.0 | 361.8 | 443.1 | 429.6 | 439.0 |
| $^{241}$Pu | 4.2 | 142.0 | 8.4 | 12.4 | 13.0 | 14.1 |
| $^{242}$Pu | -- | 87.6 | 25.2 | 65.2 | 64.9 | 85.2 |
| Total plutonium, kg : | 701.0 | 1200.0 | 1200.0 | 1200.0 | 1200.0 | 1200.0 |
| Isotopic burn-able poison composition, kg : | | | | | | |
| $^{166}$Er | 132.0 | 16.8 | 18.0 | -- | -- | -- |
| $^{167}$Er | 94.2 | 11.4 | 12.2 | -- | -- | -- |
| $^{170}$Er | 61.4 | 7.5 | 8.0 | -- | -- | -- |
| Total erbium, kg : | 293.6 | 35.7 | 38.2 | -- | -- | -- |

**Table 3.** Reactivity coefficient ($\Delta k_{eff}/\Delta T$) dependence on fuel, graphite and fuel / graphite temperature for different GT-MHR fuel cases ($\Delta k_{eff}$ expressed in pcm, and $\Delta T$ in K).

| Fuel | Pu temperature effect: $\Delta T_{Pu}$=300 K ($T_{Graphite}$=1200 K) | Graphite temperature effect $\Delta T_G$=400 ($T_{Pu}$=1500 K) | Graphite and Pu temperature effect $\Delta T_{Pu}$=300 K $\Delta T_G$=400 K |
|---|---|---|---|
| RBMK Pu1 | -3.6±0.9 | -9.2±0.7 | -12.8±1.1 |
| RBMK Pu3 | -2.4±0.9 | -9.1±0.7 | -11.5±1.1 |
| LWR Pu | -2.1±0.9 | -8.5±0.7 | -10.6±1.1 |
| Military Pu | 0.9±0.9 | -9.6±0.7 | -8.7±1.1 |

**Table 4.** Major effective macroscopic cross sections (1/cm) and effective microscopic cross sections (barns) for Military Pu as GT-MHR fuel case.

| Military Pu | $^{239}$Pu | | $^{241}$Pu | | $^{239}$Pu | | $^{240}$Pu | | $^{167}$Er | |
|---|---|---|---|---|---|---|---|---|---|---|
| Time, days | $\sigma_{fiss}$ (b) | $\boldsymbol{\Sigma_{fiss}}$ **(1/cm)** | $\sigma_{fiss}$ (b) | $\boldsymbol{\Sigma_{fiss}}$ **(1/cm)** | $\sigma_{capt}$ (b) | $\boldsymbol{\Sigma_{capt}}$ **(1/cm)** | $\sigma_{capt}$ (b) | $\boldsymbol{\Sigma_{capt}}$ **(1/cm)** | $\sigma_{capt}$ (b) | $\boldsymbol{\Sigma_{capt}}$ **(1/cm)** |
| 0 | 77 | **1.64** | 79 | **0.01** | 46 | **0.98** | 254 | **0.31** | 46 | **0.98** |
| 250 | 97 | **1.32** | 94 | **0.11** | 59 | **0.80** | 181 | **0.50** | 59 | **0.80** |
| 550 | 160 | **0.90** | 143 | **0.31** | 97 | **0.54** | 159 | **0.56** | 97 | **0.54** |

**Table 5.** Major effective macroscopic cross sections (1/cm) and effective microscopic cross sections (barns) for LWR Pu fuel case.

| LWR Pu | $^{239}$Pu | | $^{241}$Pu | | $^{239}$Pu | | $^{240}$Pu | | $^{167}$Er | |
|---|---|---|---|---|---|---|---|---|---|---|
| Time, days | $\sigma_{fiss}$ (b) | $\boldsymbol{\Sigma_{fiss}}$ **(1/cm)** | $\sigma_{fiss}$ (b) | $\boldsymbol{\Sigma_{fiss}}$ **(1/cm)** | $\sigma_{capt}$ (b) | $\boldsymbol{\Sigma_{capt}}$ **(1/cm)** | $\sigma_{capt}$ (b) | $\boldsymbol{\Sigma_{capt}}$ **(1/cm)** | $\sigma_{capt}$ (b) | $\boldsymbol{\Sigma_{capt}}$ **(1/cm)** |
| 0 | 68 | **0.85** | 70 | **0.19** | 41 | **0.51** | 107 | **0.56** | 199 | **1.74** |
| 250 | 77 | **0.68** | 76 | **0.25** | 47 | **0.42** | 109 | **0.54** | 247 | **1.19** |
| 550 | 103 | **0.53** | 97 | **0.34** | 63 | **0.33** | 113 | **0.50** | 313 | **0.61** |
| 850 | 146 | **0.33** | 130 | **0.43** | 90 | **0.21** | 132 | **0.47** | 347 | **0.26** |

**Table 6.** Major effective macroscopic cross sections (1/cm) and effective microscopic cross sections (barns) for RBMK Pu1 fuel case.

| RBMK Pu1 | $^{239}$Pu | | $^{241}$Pu | | $^{239}$Pu | | $^{240}$Pu | | $^{167}$Er | |
|---|---|---|---|---|---|---|---|---|---|---|
| Time, days | $\sigma_{fiss}$ (b) | $\Sigma_{fiss}$ (1/cm) | $\sigma_{fiss}$ (b) | $\Sigma_{fiss}$ (1/cm) | $\sigma_{capt}$ (b) | $\Sigma_{capt}$ (1/cm) | $\sigma_{capt}$ (b) | $\Sigma_{capt}$ (1/cm) | $\sigma_{capt}$ (b) | $\Sigma_{capt}$ (1/cm) |
| 0 | 69 | **1.03** | 73 | **0.01** | 41 | **0.62** | 94 | **0.64** | 188 | **1.52** |
| 250 | 78 | **0.84** | 79 | **0.13** | 47 | **0.51** | 95 | **0.63** | 243 | **1.10** |
| 550 | 99 | **0.63** | 94 | **0.27** | 60 | **0.39** | 100 | **0.60** | 298 | **0.57** |
| 850 | 139 | **0.42** | 124 | **0.40** | 85 | **0.26** | 113 | **0.56** | 353 | **0.25** |
| 950 | 158 | **0.34** | 139 | **0.44** | 97 | **0.21** | 120 | **0.54** | 408 | **0.20** |
| 1100 | 198 | **0.22** | 170 | **0.48** | 122 | **0.14** | 131 | **0.49** | 434 | **0.13** |

**Table 7.** Major effective macroscopic cross sections (1/cm) and effective microscopic cross sections (barns) for RBMK Pu3 fuel case.

| RBMK Pu3 | $^{239}$Pu | | $^{241}$Pu | | $^{239}$Pu | | $^{240}$Pu | |
|---|---|---|---|---|---|---|---|---|
| Time, days | $\sigma_{fiss}$ (b) | $\Sigma_{fiss}$ (1/cm) | $\sigma_{fiss}$ (b) | $\Sigma_{fiss}$ (1/cm) | $\sigma_{capt}$ (b) | $\Sigma_{capt}$ (1/cm) | $\sigma_{capt}$ (b) | $\Sigma_{capt}$ (1/cm) |
| 0 | 76 | **0.98** | 79 | **0.02** | 46 | **0.59** | 87 | **0.70** |
| 250 | 87 | **0.76** | 86 | **0.17** | 53 | **0.46** | 91 | **0.68** |
| 550 | 113 | **0.54** | 105 | **0.32** | 69 | **0.33** | 97 | **0.63** |
| 850 | 158 | **0.30** | 138 | **0.45** | 97 | **0.19** | 112 | **0.57** |
| 950 | 181 | **0.23** | 156 | **0.48** | 111 | **0.14** | 122 | **0.54** |

**Table 8.** The fuel and Er isotopic compositions at the end of the fuel cycle.

| Isotopic composition | Military Pu | LWR Pu | RBMK Pu1 | RBMK Pu3 |
|---|---|---|---|---|
| Fuel cycle, days | 550 | 850 | 1100 | 950 |
| Neutron fluence, n/cm$^2$ | $8.05\times10^{21}$ | $1.11\times10^{22}$ | $1.11\times10^{22}$ | $1.30\times10^{22}$ |
| Actinides | Mass, kg | | | |
| $^{237}$Np | 0.0 | >0.5 | >0.5 | >0.5 |
| $^{238}$Pu | >0.5 | 29.2 | 6.3 | 8.6 |
| $^{239}$Pu | 174.0 | 122.0 | 59.3 | 67.1 |
| $^{240}$Pu | 109.0 | 189.0 | 199.0 | 238.0 |
| $^{241}$Pu | 67.8 | 176.0 | 151.0 | 165.0 |
| $^{242}$Pu | 10.7 | 113.0 | 75.1 | 96.7 |
| $^{241}$Am | 1.8 | 9.6 | 7.3 | 7.4 |
| $^{243}$Am | 1.1 | 21.8 | 13.8 | 19.5 |
| $^{242}$Cm | 3.5 | 3.3 | 3.5 | 3.0 |
| $^{244}$Cm | >0.5 | 14.9 | 10.2 | 15.1 |
| $^{245}$Cm | 0.0 | 1.2 | 0.8 | 1.2 |
| Total | 365.5 | 680.2 | 526.5 | 621.8 |
| Burnable poison | Mass, kg | | | |
| $^{167}$Er | 19.8 | 0.9 | 0.5 | -- |

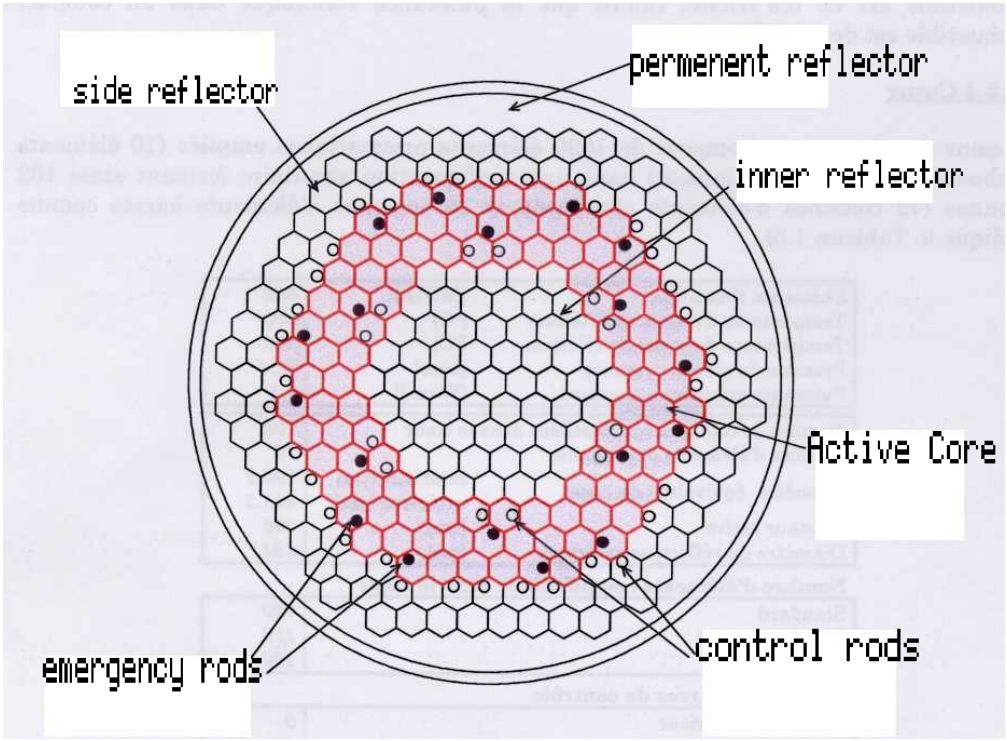


**Fig. 1.** A cross sectional view of GT-MHR reactor with hexagonal core and graphite reflectors structure. The active core is 8m high. Also see Table 1.

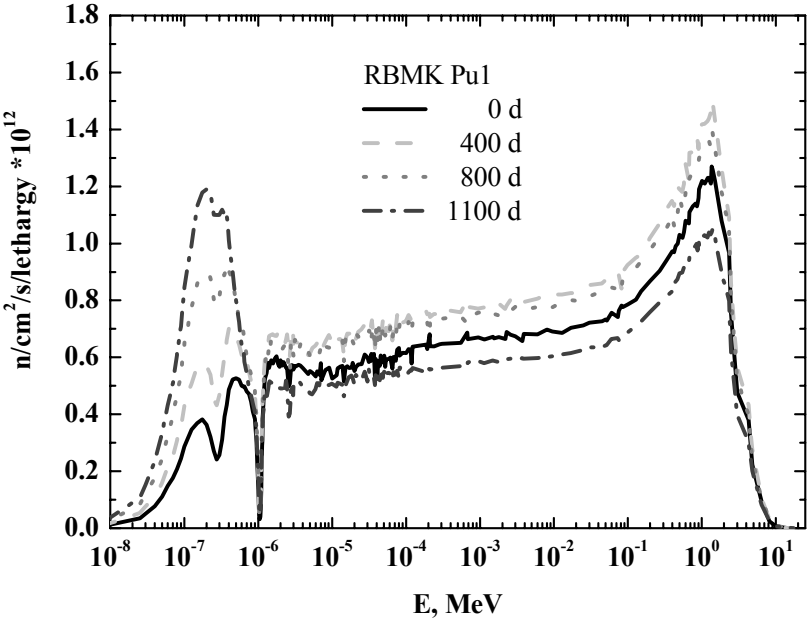


**Fig. 2.** Typical change of the average energy spectra of neutrons in the active core of GT-MHR with RBMK fuel (burn-up expressed in full power days). The thermal neutron contribution to the neutron flux varies from 9 to 22% at the beginning and at the end of the fuel cycle correspondingly.

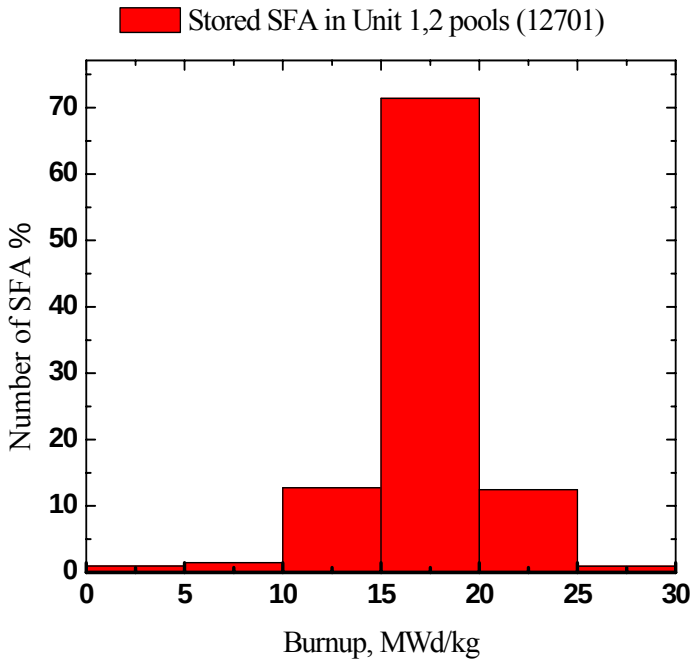


**Fig. 3.** SNF assemblies in RBMK-1500 unit 1and unit 2 storage pools. SFA stands for spent fuel assemblies.

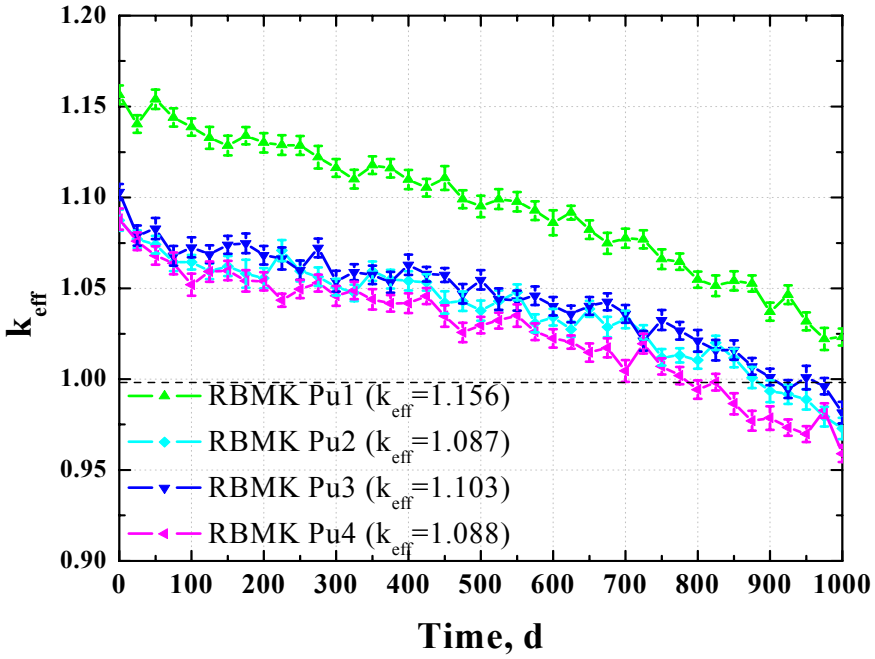


**Fig. 4.** Behaviour of $k_{eff}$ for different RBMK plutonium cases without burnable poison in GT-MHR.

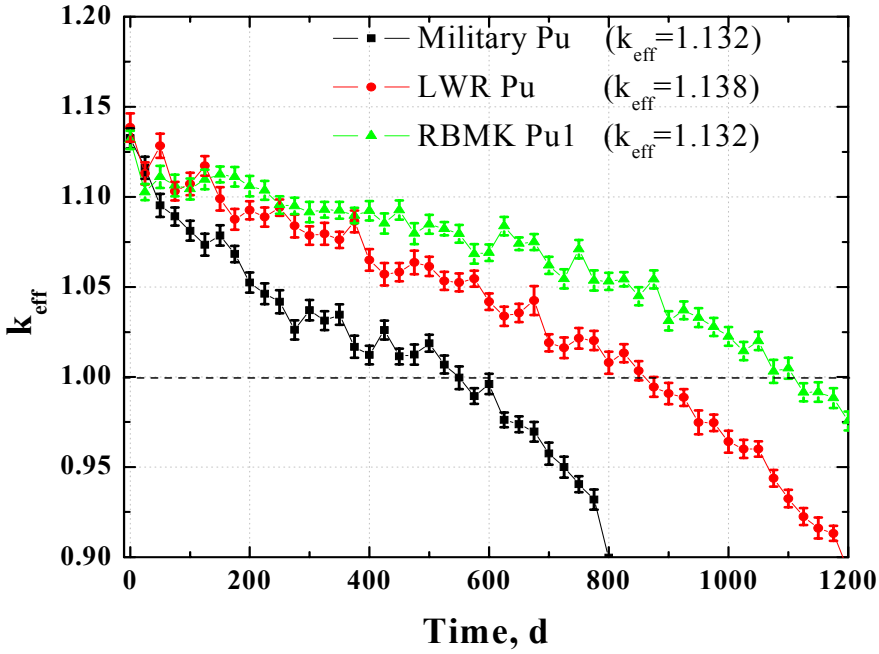


**Fig. 5.** Behaviour of $k_{eff}$ for Military, LWR and 14MWd/kg burnup RBMK plutonium (Pu1) with burnable poison in GT-MHR.

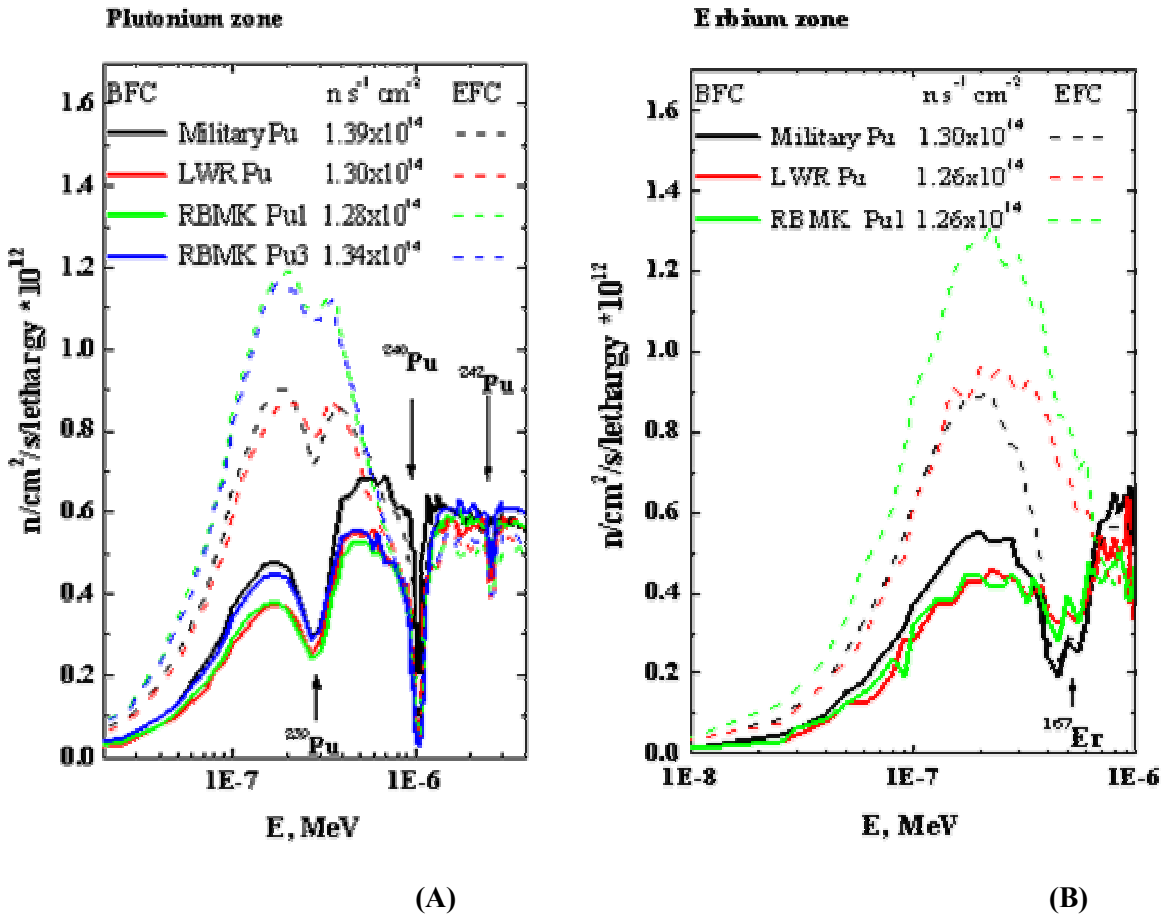


**Fig. 6. A)** Neutron flux spectrum in fuel material cells for different GT-MHR fuel cases at the beginning and at the end of the fuel cycle. **B)** Same as in (A) but in the burn-able poison cells.

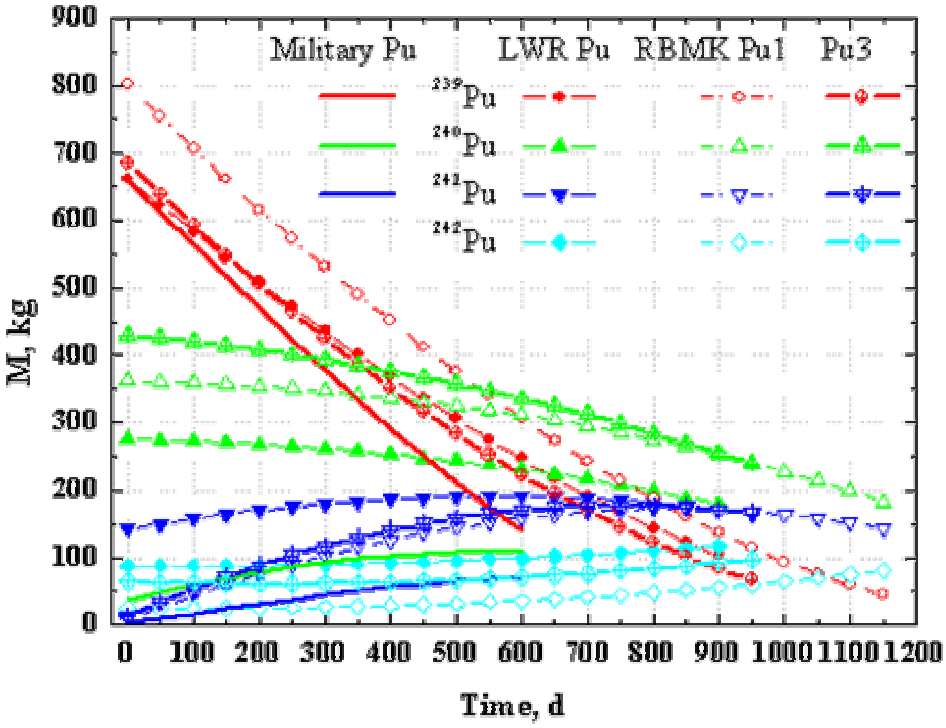


**Fig. 7**. Evolution of mass of Pu isotopes in GT-MHR loaded with different fuel: Military Pu, LWR Pu, RBMK Pu1 and RBMK Pu3 (see Table 2).